



# First-principle calculations and experimental investigation on the infrared emissivity property of Mg-doped ZnO



Tengchao Guo, Guoyue Xu, Shujuan Tan\*, Ning Liu, Jianchao Zhang, Xiangxiong Zeng, Juan Liang

College of Material Science and Technology, Nanjing University of Aeronautics and Astronautics, Jiang Jun Street 29, Nanjing 211106, China

## ARTICLE INFO

### Article history:

Received 24 March 2017

Received in revised form 1 August 2017

Accepted 4 August 2017

Available online 7 August 2017

### Keywords:

Infrared emissivity

Mg doped ZnO

Electronic properties

First-principle calculation

## ABSTRACT

The electronic properties and infrared emissivity of  $Zn_{1-x}Mg_xO$  ( $x = 0, 0.0625, 0.125$ ) were systematically investigated by using the first-principle calculations based on density functional theory (DFT). The  $Zn_{1-x}Mg_xO$  ( $x = 0, 0.0625, 0.125$ ) powders were prepared by sol-gel method and their infrared emissivity in the wavelength of 8–14  $\mu\text{m}$  was characterized. The results indicate that the infrared emissivity increases with the increase in Mg concentration, which is attributed to the reduction in conductivity and in the real part of dielectric function. Furthermore, the variation in conductivity and dielectric function has been well studied, and a reasonable method to calculate infrared emissivity of semiconductors has been established. It is expected that this method can be used for designing materials with different infrared emissivity and also applied for effectively guiding the experimental investigation.

© 2017 Published by Elsevier Ltd.

## 1. Introduction

In recent years, semiconductor materials have received increasing attention because of their widespread applications. Infrared emissivity is an important property of semiconductors as it determines the thermal radiation behavior of materials. Semiconductor materials with either high or low infrared emissivity are widely used in both military and civilian fields. For example, high infrared emissivity materials are used in light emitting diodes (LEDs) and the surface of satellites for heat dissipation [1,2], and also in tunnel kilns and electric furnaces for energy-saving [3]. Low infrared emissivity materials could be used in solar collector systems, and military camouflage targets [4].

Due to their extensive applications in both military and civilian fields, many research activities have been carried out to investigate the infrared emissivity of semiconductor materials in the last decades. For instance, Wang et al. [5] investigated the infrared emissivity of  $BaO-Al_2O_3-SiO_2$  (BAS) and Sr-doped BAS (BSAS), and reported that the variation of infrared emissivity was due to the different crystalline structures. Mao and coworkers [6] studied the infrared emissivity of Al-doped ZnO and La-doped ZnO, and found that the variation of infrared emissivity was due to the differences in particle size, free electrons and scattering of infrared photons.

Zhang et al. [7] reported that Mn-doped ZnO:Co powders possess different infrared emissivity values because of differences in crystalline quality and resistivity. Wang and Tian et al. [8,9] demonstrated that the infrared emissivity of  $Al_2O_3/Cr_2O_3$  was related to the lattice absorption, and that the infrared emissivity value of  $TiO_2$  was possibly due to the photon emission from the as-formed  $TiO_2$  phase. Lee et al. [10] noted that the infrared emissivity of Ti-based oxides was associated with band structure of semiconductor materials. Huang et al. [11–13] investigated the infrared emissivity of  $CeO_2$  and La-doped  $CeO_2$  and found that the variation of infrared emissivity was due to surface roughness and cauliflower-like microstructures which caused multiple reflections and coupling between incident electromagnetic waves and surface polarizations.

The previous studies on infrared emissivity of semiconductor materials are mainly based on the experimental findings. However, to the best of our knowledge, few studies have been reported on the theoretical calculations of the semiconductors' infrared emissivity. Such studies would be significant as they can be used for further explaining and predicting the experimental results.

As is known, zinc oxide (ZnO) is a wide band gap II-VI semiconductor with hexagonal wurtzite structure and owns a large exciton binding energy (60 meV). Therefore, ZnO has excellent optical and electrical properties, and shows great potential for application in many fields, such as solar cells, gas sensors, photocatalysis, and even in microwave and infrared compatible stealth materials [14–16]. In this paper, the theoretical

\* Corresponding author.

E-mail address: [tanshujuan@nuaa.edu.cn](mailto:tanshujuan@nuaa.edu.cn) (S. Tan).

infrared emissivity values of Mg-doped ZnO with different Mg doping concentrations in the wavelength of 8–14  $\mu\text{m}$  have been calculated by employing the first principles plane-wave pseudo-potential method. The calculated results have also been compared with the corresponding results from experimental measurements.

## 2. Computational details

### 2.1. Theoretical models

The ideal ZnO has a hexagonal wurtzite structure with space group symmetry of P63mc. The lattice parameters of ZnO crystal cell are  $a = b = 0.3249 \text{ nm}$ ,  $c = 0.5205 \text{ nm}$ ,  $\alpha = \beta = 90^\circ$ , and  $\gamma = 120^\circ$  [17,18]. To study the effect of Mg dopant concentration (0, 6.25, 12.5 at.%) on the infrared emissivity of ZnO, two supercell models of Mg-doping ( $2 \times 2 \times 2$ ) and ( $2 \times 2 \times 1$ )  $\text{Zn}_{1-x}\text{Mg}_x\text{O}$  are constructed. To simulate Mg-doped ZnO crystalline structure for different doping concentrations, one Zn atom is substituted with one Mg atom in the two supercell models. The dopant concentrations of Mg are 0, 6.25, and 12.5 at.%, and the supercell models are shown as Fig. 1.

### 2.2. Computational method

The ab initio calculations were carried out by using CASTEP package (MS6.1, Accelrys Company) which is based on density functional theory (DFT). The structure optimization was performed by using the generalized gradient approximation (GGA) method. The interaction between ions and valence electrons was described by ultrasoft pseudopotential (USP) and the exchange-correlation energy was described by Perdew-Burke-Ernzerhof (PBE) functional [19]. The constructed valence-electron configurations are  $\text{Zn}3d^{10}4s^2$ ,  $\text{Mg}2p^63s^2$ , and  $\text{O}2s^22p^4$ , respectively. After careful testing, the cutoff energy was set to 400 eV and the k-point set mesh was chosen to be  $5 \times 5 \times 4$ . For the geometry optimization process, the energy change and the maximum tolerances of the force, stress, and displacement were set to  $1 \times 10^{-6} \text{ eV/atom}$ , 0.03 eV/Å, 0.05 GPa and 0.001 Å, respectively. Electrons were treated by spin polarization and bandgap was modified by GGA+U method.  $U_{d,\text{Zn}} = 10.0 \text{ eV}$  for Zn 3d and  $U_{p,\text{O}} = 7.0 \text{ eV}$  for O 2p were adopted in the GGA+U method [20].

## 3. Experimental methods

### 3.1. Materials

Zinc nitrate hexahydrate ( $\text{Zn}(\text{NO}_3)_2 \cdot 6\text{H}_2\text{O}$ ), Magnesium nitrate hexahydrate ( $\text{Mg}(\text{NO}_3)_2 \cdot 6\text{H}_2\text{O}$ ), Anhydrous ethanol ( $\text{C}_2\text{H}_5\text{OH}$ ), Sodium hydroxide (NaOH). Deionized water was used throughout

the experiments. Zinc nitrate hexahydrate and Magnesium nitrate hexahydrate were purchased from Aladdin chemicals Company, China. Anhydrous ethanol and Sodium hydroxide were purchased from Nanjing chemical agent limited company, China. All the solvents were analytical reagent grade and used without further purification.

### 3.2. Preparation of ZnO and Mg-doped ZnO particles

Un-doped and doped  $\text{Zn}_{1-x}\text{Mg}_x\text{O}$  ( $x = 0, 0.0625, 0.125$ ) particles were prepared by sol-gel method. In a typical procedure, 0.05 mol  $\text{Zn}(\text{NO}_3)_2 \cdot 6\text{H}_2\text{O}$  and  $\text{Mg}(\text{NO}_3)_2 \cdot 6\text{H}_2\text{O}$  were firstly dissolved in 100 mL of deionized water, and the molar ratio of  $\text{Mg}(\text{NO}_3)_2 \cdot 6\text{H}_2\text{O}$  was 0, 0.0625 and 0.125 respectively. In a separate flask, 0.1 mol NaOH was dissolved in 100 mL of deionized water. Then, the NaOH solution was added drop-wise to the metal nitrate solution and a white gel was formed gradually. This gel was kept at room temperature for 12 h to settle down. Then, the precipitates were filtered, and washed with deionized water and  $\text{C}_2\text{H}_5\text{OH}$  several times. Finally, they were dried in a hot air oven at  $80^\circ\text{C}$  for 10 h and calcined at  $550^\circ\text{C}$  for 2 h to yield the un-doped and Mg-doped ZnO particles.

### 3.3. Characterization

Infrared emissivity values of coatings in the wavelength of 8–14  $\mu\text{m}$  were measured by an IR-2 Infrared Emissometer (Shanghai Institute of Technological Physics, China), and the measurement error was less than 0.001. The emissivity values were obtained by averaging over the data measured from three different regions of each coating at room temperature. The emissivity test principle and method are described in a previous work [21].

## 4. Result and discussion

### 4.1. Structural parameters

The equivalent lattice parameters of the hexagonal wurtzite structures of un-doped and Mg-doped ZnO after geometry optimization are shown in Table 1. As described in Table 1, the lattice parameters of pure ZnO are  $a = 3.2808 \text{ \AA}$  and  $c = 5.3139 \text{ \AA}$ , which are consistent with the experimental results and other theoretical calculated results [22]. After ZnO is doped with Mg, the lattice parameter  $a$  is found to increase, whereas  $c$  parameter is found to decrease with increase in Mg content in ZnO. This phenomenon could be explained as follows [23]: the ionic radius of  $\text{Mg}^{2+}$  (0.065 nm) is smaller than that of  $\text{Zn}^{2+}$  (0.074 nm), thus, the replacement of  $\text{Zn}^{2+}$  by  $\text{Mg}^{2+}$  decreases the lattice parameter  $c$ . In addition, the difference in electronegativity between Zn and Mg

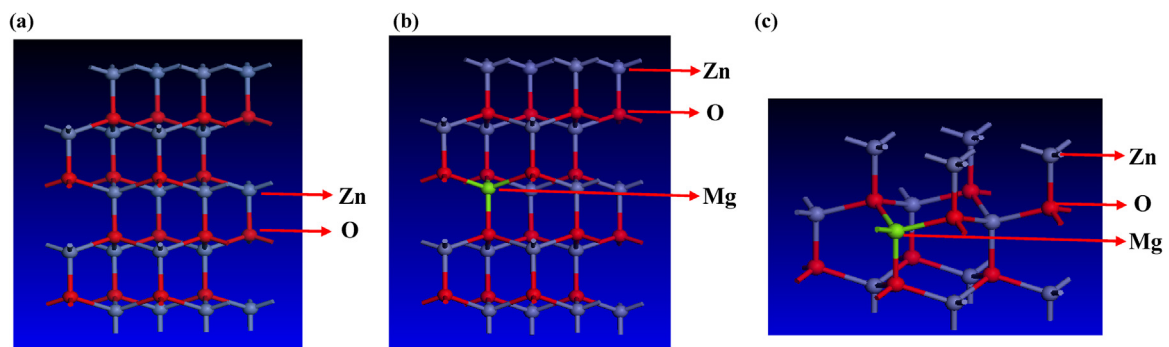


Fig. 1. Supercell models:(a)  $2 \times 2 \times 2$  supercell of ZnO, (b)  $2 \times 2 \times 2$  supercell of ZnO doped with 6.25 at.% Mg, (c)  $2 \times 2 \times 1$  supercell of ZnO doped with 12.5 at.% Mg.

Download English Version:

<https://daneshyari.com/en/article/5441822>

Download Persian Version:

<https://daneshyari.com/article/5441822>

[Daneshyari.com](https://daneshyari.com)